PCI/NATIONAL BRIDGE CONFERENCE 2006

A Comparative study of Creep & Shrinkage Models for HPC Prestressed Members

Topic area: LRFD Issues, Research, **Paper #43**

by

Walter D. Mesía

Graduate Research Assistant
Civil and Environmental Engineering Department
The George Washington University
Washington DC, USA

and

Sameh S. Badie, Ph.D., P.E.

Assistant Professor
Civil and Environmental Engineering Department
The George Washington University
Washington DC, USA

Introduction

Along its service life, concrete suffers continuous changes of its volume, due to the applied loads and the inherent creep and shrinkage properties. Creep and shrinkage effects are more critical in concrete structures used to resist axial compressive loads, such as prestressed structures. In this type of structures, the effect of creep and shrinkage added to the relaxation of the prestressed tendons continuously reduces the prestressing force along the service life of the structure, which directly reduces its flexural capacity.

Another application where creep and shrinkage strains have significant effect is the composite concrete slab/beam construction system for continuous span structures. This system is widely used in highway bridges as it produces stiffer structures with longer spans and/or wider girder spacing. In this type of construction, precast prestressed concrete beams are installed as simply supported beams between supports and then a cast-in-place slab is cast on top of them. Continuity reinforcement for the negative moment zones at intermediate supports is installed in the slab. Over time, the beam concrete creeps under the prestressing force causing the beam to deflect upward as shown in Figure 1-a. Since the beam ends are locked by continuity of the composite superstructure, a positive moment is developed as shown in Figure 1-a. At the same time, while the concrete beam creeps, differential shrinkage between the beam and slab occurs. This differential shrinkage occurs due to the fact that when the slab is cast, the beams have already got rid of most of their shrinkage deformation, whereas the slab has yet to shrink. With the shrinkage of the slab concrete exceeding that remaining in the beam concrete, the composite slab/beam structure deflects downward producing negative moment at the intermediate supports as shown in

Figure 1-b. In most cases, the positive moment that occurs due to creep of the beam exceeds that occur due to differential shrinkage between the slab and beam. This results in a net positive restraining moment as shown in Figure 1-c that tends to reduce continuity.

Figures 1-d, 1-e and 1-f show the effect of the restraining moment on a three-span continuous beam structure. Based on the value of the positive restraining moment, (Figure 1-e), with respect to the total moment due to the applied load (Figure 1-d), the superstructure may end up behaving as a series of simply supported beams with zero negative moment at interior supports, as shown in Figure 1-f. If not carefully taken into consideration, restraining moments due to creep and shrinkage of continuous span structures can increase the positive moment demand and make the system structurally unsafe. This type of behavior has been the focus of many researchers over the past 30 years. Reference 1 provides a good summary of the literature on this issue.

Until 1994, designers used to use the following models to estimate creep and shrinkage strains: (1) ACI-209[2] model recommended by the American Concrete Institute and (2) the CEB 1990 Model Code[3]. These models were originally developed in 1970s and 1980s, respectively, based on concrete mixes with a maximum compressive strength at 28 days of about 5 to 6 ksi (34.4 to 41.4 MPa).

In 1994, the American Association of State Highway and Transportation officials released the first edition of the AASHTO LRFD specifications[4] that provided a detailed model for calculating creep and shrinkage strains for reinforced concrete members. This model was developed in the 1980s by Collins and Mitchell[5], Rusch et al[6], Bazant and Wittman[7], and Ghali and Favre[8], using concrete mixes with a maximum concrete strength of about 7 ksi (48.3 MPa). The same model has continued to appear in successive editions of the LRFD specifications (1998[9] and 2004[10]). Recently, new models that predict creep and shrinkage effects have been developed such as the model given by the PCI-Bridge Design Manual[11] and the model developed in the NCHRP 18-07[12]. These models were developed for the use of high-performance concrete (HPC) mixes.

It is worthy to mention that the ACI-318 building code, until its recent edition (ACI-318-05[13]), does not provide in its main body any detailed model to determine the creep and shrinkage effects. However, the commentary of section 18.6 of the ACI-318-05[13] guides the reader to use the model developed by Zia and his associates[14]. The authors of this paper investigated Zia's model and found that the main creep and shrinkage models are similar to those provided in the AASHTO-LRFD[9] specification. Therefore, Zia's model was not considered for further investigation in this study.

The majority of the software available in the market, that gives the designer the availability to account for creep and shrinkage effects, provides only three models in their coding, which are the ACI-209[2], CEB 90[3], and AASHTO LRFD 1998[9]. However, the software leaves the choice of using any of these models to the designer's discretion

without giving any recommendations or even a short background on the criteria used to develop them.

This paper presents the results of a parametric study conducted to study the creep and shrinkage effects on prestressed members using the following models: ACI 209[2], CEB 90[3] and AASHTO LRFD 1998[9]. The objective of the study is to show the diversity of results between the three models, especially at high concrete compressive strength. Also, the study tries to investigate if the geometrical properties of the prestressed girders, used with the concrete slab/beam construction systems, have effect on the final results. Two structures were investigated in the parametric study. The first structure is a 100-ft (30.48 m) long column subject only to concentric axial prestress force. The second structure is a continuous 3-span prestressed concrete slab/beam bridge.

Creep and Shrinkage Models used in the Study

ACI 209

This model was developed in early 1970s based on the research findings that were available at that time. It was developed under the ACI 209[2] committee. However, it has never been included in the ACI 318 building code or any other code or specifications. It is very important to remember that this model was developed at a time where the maximum concrete strength was about 5 to 6 ksi, (34.4 to 41.4 MPa).

CEB 1990

This model was included in this study to represent one of the reliable models that has been widely used across the globe. It was developed based on extensive research conducted in Europe in the 1970s and 1980s. It is worthy to mention that this model has not been used extensively in the United States. That is because it is based on research that was conducted in Europe using aggregate with properties that may be different from those of the aggregate used in the United States.

AASHTO-LRFD 1998

This model appeared for the first time in the first edition of the AASHTO LRFD specifications (1994[4]) based on the research conducted in the 1980s by Collins and Mitchell[5], and many other researchers[6,7,8]. At that time (1994), it was considered a more refined model than the ACI 209[2] model as it recognized a larger number of factors that affect creep and shrinkage behavior. Also, it opened the way for design engineers to have a second source to compute creep and shrinkage effects besides the ACI 209[2] model. This model has continued to appear in successive editions of the LRFD specifications (1998[9] and 2004[10]). The model as appeared in the second edition of the LRFD specifications (1998[9]) is considered in this study.

Table 1 gives a summary of the three models and Table 2 gives a summary of the notations used with these models.

Parametric study

Two cases are used to compare between the three models of creep and shrinkage considered in this study. A spread sheet was developed by the researchers to conduct the parametric study. Also, a commercial software[15] was used to verify the accuracy of the spread sheet. The creep and shrinkage effects were calculated by dividing the time line into discrete intervals each with a finite amount of time. For each interval, the material properties as well as the creep and shrinkage properties of various concrete parts of the structure were determined at the starting point of the interval. Then the creep and shrinkage strains were determined for this interval and added to the total strains determined by the end of the previous interval.

Case study #1:

A 100 ft (30.48m) long column with a 12x12 in (0.305x0.305 m) square cross section was used. To reduce the parameters that may affect the results, the weight of the column as well as the buckling effects were ignored in the analysis. The column was reinforced with 4 – ½" (12.7 mm) diameter, low relaxation, 270 ksi (1.86 GPa) strands made concentric with the column cross section. No external load was applied on the column. The stress in the strands just before release was 0.75 f_{pu} = 202.5 ksi (1.40 GPa). The column was analyzed over a period of 10,000 days, considering the time of releasing the prestress force as time zero. The 10,000 days period was divided into the following intervals: 1, 2, 3, 4, 5, 6, 7, 15, 30, 60, 90, 120, 150, 300, 500, 1000, 1500, 2000, 2500, 5000, and 10,000 days. The analysis was conducted using a spread sheet developed by the authors. The accuracy of the spread sheet was confirmed by comparing its results with a commercial software[15]. The following parameters were considered in the parametric study:

a. Concrete strength at 28 days, f_c': Three values of f_c' were used 5, 10 and 15 ksi. This range enables the authors to cover normal strength concrete mixes as well as high performance concrete mixes.
b. Creep and shrinkage models: ACI-209[2], CEB-90[3], LRFD 1998[9].
c. Level of non-prestressed reinforcement as a percentage of the prestressing reinforcement, three levels are used: Zero, 130.7% (4#4 bars), 513.1% (4#8 bars). Please, note that the bars are set concentric with the column cross section. This parameter was considered in the study because, in many cases, non-prestressed reinforcement is used in prestressed members for serviceability purposes such as crack and deflection control, or for fabrication purposes such as stirrup hangers.

Case study #2:

A continuous three-span composite slab/I-beam bridge was analyzed using the three available models (ACI-209[2], CEB-90[3], LRFD 1998[9]). The bridge was 56ft (17.07 m) wide and the superstructure consisted of 6 beams spaced at 10 ft (3.05 m) supporting an 8-in (203.2 mm) thick slab with a 2-in (50 mm) thick concrete wearing surface. The concrete

strength of the beams was 5.6 and 7.0 ksi (38.61 and 48.26 MPa) at release and 28 days, respectively.

The cast-in-place slab had a 28-day concrete strength of 3.0 ksi (20.68 MPa). The ratio between the end-span to the center-span was taken 90%. In order to cover a wide range of practical cases in this example, the following parameters expected to affect the restraining moment due to creep and shrinkage effects were considered:

a. The girder type: three different type of I girders were used. These were the Bulb Tee BT-72, NU-1800 I girder, and Washington Super Girder W74G. These types were chosen because they represent about 70% or more, of all the I-girder types used across the country. The length of the center span of the bridge is optimized for each beam type. The optimization process was made by ignoring the creep and shrinkage effects and using the following criteria:
    - The precast girders are installed as simply supported beams.
    - The weight of the cast-in-place slab is supported by the simply supported beams.
    - Continuity of the superstructure is achieved after the slab is hardened. Therefore, the superimposed dead and live loads are supported by the composite continuous superstructure.
    - AASHTO-LRFD live load model, HL-93, is used in the design.
    - The beams are designed to have adequate capacity for vertical shear and flexural effects.
b. Age of the girder at time of continuity was created: Some of the state highways agencies recommend that continuity should not be established before the girders are 90-day old, otherwise, creep and shrinkage effects should be investigated. This is because the older the girders are at time of creating continuity, the lower the restraining moment will be. However, it has been recorded in the literature[1] that girders as young as 30-days old were used when continuity was established. In this study, three ages were considered 30, 60, 90 days, to cover all possible cases.

The time dependent analysis considering the creep and shrinkage effects was conducted using a commercial software[15]. The analysis was conducted for a period of 10,000 days starting from the time of installing the girders using the time plan showed on Table 3.

Discussion of results

Case study #1: 100-ft long column:

Figures 2 to 4 shows a summary of the results of the investigation. In each figure the amount of effective prestress as a percentage of f_{pu} is plot against time. From these figures, the following conclusions can be drawn.

- Regardless the concrete strength and the amount of non-prestressed reinforcement, the CEB-90[3] model always gives higher initial losses (due to elastic shortening), than the ACI-209[2] and LRFD 1998[9] models, while the ACI-209[2] and LRFD 1998[9] models give almost the same amount of initial losses.
- At low f_c' (5 ksi, 34.47 MPa) the CEB-90[3] model shows higher final losses than the LRFD 1998[9] model, and the LRFD 1998[9] model gives higher final losses than the ACI-209[2] model. At high f_c' (10 and 15 ksi, 68.95 and 103.42 MPa), the three models give very close values of final losses
- Adding non-prestressed reinforcement reduces the prestress losses. However, the effect of the non-prestressed reinforcement of prestress losses is more pronounced with low strength concrete.
- It is clear that after about 3 months, the CEB-90[3] model gives almost a linear rate of prestressing losses, while the ACI-209[2] and LRFD 1998[9] models, show a parabolic rate.
- The researchers believe that the parabolic distribution of prestress loss (given by the ACI-209[2] and LRFD 1998[9] models) is more convincing. This is because most of the creep and shrinkage deformation occur during the first six month of age of concrete and slow down afterward.
- The linear distribution of the prestress loss of the CEB-90[3] model is more pronounced at high f_c'(15 ksi, 103.42 MPa) than low f_c'(5 ksi, 34.47 MPa).
- The ACI-209[2] and LRFD 1998[9] models give very close results at any age, when high concrete strength is used (f_c'= 10 to 15 ksi, 68.95 to 103.42 MPa), while at low concrete strength (5 ksi, 34.47 MPa), the two models show some inconsistency beyond 100 days.
- The three models give close amount of losses between 30 to 100 days. Since installation of the precast elements in the field is usually about that age, a lump-sum value for total losses can be established to estimate losses of prestressed at time of installation. This lump sum value can be used by the designer to estimate how much prestress is left in the member at this stage and estimate the corresponding camber.

Case study #2: Continuous three-span bridge:

Figures 5, 6 and 7 give the moment at the midpoint of the center span of the bridge against the time life of the structure. The midpoint moment is given as a percentage of the difference between the full continuity moments with creep and shrinkage effects and the simple span moment. Time zero represents the time when continuity is created. Positive percentage means increase in the positive moment at midpoint of the center span. Each figure gives the results for three ages of the precast beam at time of creating continuity; 30, 60, and 90 days. Each set of curves gives a comparison between the results of the three creep and shrinkage models. By studying these figures, the following conclusions can be drawn:

- Regardless the age of girder at time of creating continuity, the creep and shrinkage model used, and the beam type, the effect of creep of the precast beam dominates the behavior over the effect of differential shrinkage effect between the deck and the beam. This type of behavior results in positive restraining moment at all interior support.
- About 80 and 95 percent of the total restraining moment due to creep and shrinkage effects is generated during the first 500 and 1000 days, respectively, after continuity is created.
- The age of the beam when continuity is created has a great effect on the magnitude on the net restraining moment. For example, the 30-day old beams showed about 30 percent increase in restraining moment over the 90-day old beams. This type of behavior has been consistently shown by other researchers[1]. This observation explains the guidelines mandated by some highway authorities that the beams have to be 60-day or older when the deck slab is cast to reduce the restraining moment.
- Regardless the beam age and type, the LRFD 1998[9] model has produced the highest restraining moment. While the ACI-209[2] model has produced the lowest restraining moments. The difference between the highest and lowest restraining moment was about 20 percent. Although, the LRFD 1998[9] model provides the most conservative estimate of the creep and shrinkage effects, using this model will lead to a significant increase in the positive moment that may force the design engineer to use shorter span, smaller girder spacing and/or deeper beam.
- The ACI-209[2] and LRFD 1998[9] models have shown a continuous-increase trend in the restraining moment, while the CEB-90[3] model has shown a reversible behavior that starts at about 5000 days, where the restraining moment started to drop down. This type of behavior means that at that age, 5000 days, the differential shrinkage between the deck and the beam started to dominate over the creep effect of the precast beam. The drop in the restraining moment was more pronounced with the NU1800 girder than the BT72 and W74G girders.
- The NU1800 girder has shown smaller restraining moment than the BT72 and W74G girders by about 10 percent. The researchers believe that this difference in behavior is due to the amount of prestressing force that is presented in each type of beams.

Conclusions

The use of high performance concrete (HPC), with members subjected to high axial forces, such as columns and prestressed members is recommended because of the reduced deformation due to creep and shrinkage effects.

Many models for creep and shrinkage effects have been developed during the past 30 years among them are the ACI-209[2], CEB-90[3] and the LRFD 1998[9] models. The two cases considered in this study have shown that there is a relatively mild diversity of the results between the three models. The diversity of results is not only related to the parameters of the creep and shrinkage model used in the analysis, but also due to the nature

and parameters of the problem being analyzed. These parameters include, concrete strength (normal strength versus high performance concrete), existence of non-prestressed reinforcement, type of beam used, and age of girder when continuity is created.

The study shows that in general, the LRFD 1998[9] model gives the most conservative results. It is recommended that the design engineer runs the analysis using all creep and shrinkage models available by the analysis tool to get a sense of the behavior. Final decision of choosing the creep and shrinkage model should be done based on studying the design criteria of available models and previous experience.

Acknowledgment

The researchers would like to provide their thanks to Lee Tanase, Vice-president of LEAP Software, Inc. for providing the analytical tool that is used to conduct this study. Also the researchers would like to thank the Civil and Environmental Engineering Department of the George Washington University for providing the financial support to conduct this study.

References

1. McDonagh, M., and Hinkley, K., "Resolving Restraint Moments: Designing for Continuity in Precast Prestressed Concrete Girder Bridges", Prestressed/Precast Concrete Institute (PCI) Journal, July-August 2003, Vol. 48, No. 4, pp. 104-119.
2. ACI Committee 209, "Prediction of Creep, Shrinkage, and Temperature Effects in Concrete Structures", (ACI 209R-92), American Concrete Institute, Farmington Hills, MI, 1992.
3. CEB 1990, CEB-FIP Model Code for Concrete Structures, Comite Euro-International du Beton, (available from Lewis Brooks, 2 Blagdon Road, New Malden, Surrey, KT3 4AD, England).
4. AASHTO LRFD Bridge Design Specifications, First Edition, American Association of State Highway and Transportation Officials, Washington DC, 1994.
5. Collins, M.P., and Mitchell, D., "Prestressed concrete structures", Englewood Cliffs, N.J., Prentice Hall, 1991.
6. Rüsch, H., Jungwirth, D. and Hilsdorf, H., "Creep and Shrinkage: their effect on the behavior of concrete structures", New York, Springer-Verlag, 1983.
7. Bazant, Z.P. and Wittmann, F.H., "Creep and Shrinkage in concrete structures", Chichester; New York, Wiley, 1982.
8. Ghali, A., and Favre, R., "Concrete structures: stresses and deformations", London, New York, Chapman and Hall, 1986.
9. AASHTO LRFD Bridge Design Specifications, Second Edition, American Association of State Highway and Transportation Officials, Washington DC, 1998.
10. AASHTO LRFD Bridge Design Specifications, Third Edition, American Association of State Highway and Transportation Officials, Washington DC, 2004.

11. PCI Bridge Design Manual (BDM), Prestressed/Precast Concrete Institute (PCI), Chicago, Illinois, 1997.
12. NCHRP 18-07, Tadros. M. K., "Prestress Losses in Pretensioned High-Strength Concrete Bridge Girders," National Cooperatives Highway Research Program, Washington DC, 2002.
13. ACI 318-05, "Building Code Requirements for Structural Concrete", American Concrete Institute, Farmington Hills, MI, 2005.
14. Zia, P; Preston, H.K.; Scott, N.L.; and Workman, E.B., " Estimating Prestress Losses", Concrete International: Design & Construction, V.1, No. 6, June 1979.
15. LEAP Software, Inc., Tampa, FL, 2001.

Table 1 – Creep and Shrinkage Models

Model	ACI	LRFD	CEB
Compressive strength	$(f_c')_t = \frac{t}{a+\beta_t t}(f_c')_{28}$ (psi)	$(f_c')_t = \frac{t}{a+\beta_t t}(f_c')_{28}$ (psi)	$f_{cm}(t) = \beta_{cc}(t) f_{cm}$ (Mpa) $\beta_{cc}(t) = \exp\left(s\left[1-\left(\frac{28}{t/t_1}\right)^{1/2}\right]\right)$
Modulus of Elasticity at time *t*	$E_{ct} = g_{ct}\left[w^3 (f_c')_t\right]^{1/2}$ (psi) $g_{ct} = 33.0$	$E_c = g\left(w_c^{1.5}\right)\sqrt{f_c'}$ (psi) $g = 33000$	$E_{ci}(t) = \beta_E(t) E_{ci}$ (MPa) $\beta_E(t) = [\beta_{cc}(t)]^{0.5}$
Creep Coefficient	$\upsilon = \upsilon_u(\gamma_{la})(\gamma_\lambda)(\gamma_{VS})\frac{t^{0.6}}{10+t^{0.6}}$ $\gamma_{la} = 1.25(t_{la})^{-0.118}$ (moist cured) $\gamma_{la} = 1.13(t_{la})^{-0.094}$ (steam cured) $\gamma_\lambda = 1.27 - 0.0067\lambda$, $\lambda > 40$ $\gamma_{VS} = 1.14 - 0.09(V/S)$ $\upsilon_u = 2.35$	$\psi(t,t_i) = 3.5 k_c k_f (1.58 - \frac{H}{120}) t_i^{-0.118} \frac{(t-t_i)^{0.6}}{10+(t-t_i)^{0.6}}$ $k_c = \left[\frac{26e^{\frac{t}{0.36(V/S)}}+t}{\frac{t}{45+t}}\right]\left(\frac{1.80+1.77e^{-0.54(V/S)}}{2.587}\right)$ $k_f = \frac{1}{0.67+\left(\frac{f_c'}{9}\right)}$	$\phi(t,t_o) = \phi_o \beta_c(t-t_o)$ $\phi_o = \left[\frac{5.3}{(f_{cm}/10)^{1/2}}\right]\left(1+\frac{1-RH/100}{0.46(V/50S)^{1/3}}\right)\left[\frac{1.0}{0.1+t_o^{0.2}}\right]$ $t_o = t_{o,T}\left[\frac{9}{2+(t_{o,T})^{1.2}}+1\right]^\alpha \geq 0.5 days$ $t_{o,T} = \sum_{i=1}^{n} \Delta t_i \exp\left[13.65 - \frac{4000}{273+T(\Delta t_i)}\right]$ $\beta_c(t-t_o) = \left[\frac{(t-t_o)}{\beta_H+(t-t_o)}\right]^{0.3}$ $\beta_H = 150\left[1+\left(1.2\frac{RH}{RH_o}\right)^{18}\right]\frac{h}{100}+250 \leq 1500$ $h = 2A_c/u = 2V/S$ (mm)
Shrinkage Coefficient	$\varepsilon_{sh} = 0.78x10^{-3}(\gamma_{vs})(\gamma_\lambda)(\gamma_t)$ $\gamma_{vs} = 1.2e^{(-0.12V/S)}$ $\gamma_\lambda = 1.40 - 0.01\lambda$, $\gamma_\lambda \leq 80$ $\gamma_\lambda = 3 - 0.03\lambda$, $\gamma_\lambda > 80$ $\gamma_t = \frac{t}{35+t}$, (moist cured) $\gamma_t = \frac{t}{55+t}$, (steam cured)	$\varepsilon_{sh} = -k_s k_h\left(\frac{t}{35+t}\right)0.51x10^{-3}$, (moist cured) $\varepsilon_{sh} = -k_s k_h\left(\frac{t}{55+t}\right)0.56x10^{-3}$, (steam cured) $k_s = \left[\frac{26e^{\frac{t}{0.36(V/S)}}+t}{\frac{t}{45+t}}\right]\left(\frac{1064-94(V/S)}{923}\right)$ $k_h = \left[\frac{140-H}{70}\right]$	$\varepsilon_{cs}(t,t_s) = \varepsilon_{cso}\beta_s(t-t_s)$ $\varepsilon_{cso} = \varepsilon_s(f_{cm})\beta_{RH}$ $\varepsilon_s(f_{cm}) = [160+10\beta_{SC}(9-)]x10^{-6}$ $\beta_{RH} = -1.55\beta_{sRH}$, $40\% \leq RH < 99\%$ $\beta_{RH} = +0.25$, $99\% \geq RH$ $\beta_{sRH} = 1-(RH/RH_o)^3$ $\beta_s(t-t_s) = \left[\frac{(t-t_s)}{350(h/100)^2+(t-t_s)}\right]^{0.5}$

Table 2 – Summary of Notations of the creep and shrinkage models

Symbol	Description							
I	Cement Type I, (Normal Cement)							
III	Cement Type III, (High Early Strength Cement)							
RS	Rapid hardening high strength cement							
N	Normal cements							
R	Rapid hardening cements							
SL	Slowly hardening cements							
a β_t	Compressive strength factors		Moist Cured		Steam Cured			
			I	III	I	III		
		a	4	2.3	1	0.7		
		β_t	0.85	0.92	0.95	0.98		
A_c	Area of the concrete section							
$\beta_{cc}(t)$	Concrete age coefficient							
α β_{SC}	cement type factor		RS	N	R	SL		
		α	1	0	0	-1		
		β_{SC}	8	5	5	4		
$\phi(t,t_o)$, υ , $\psi(t,t_i)$	Creep coefficient							
ε_{sh} , ε_{cs}	shrinkage coefficient factor							
E_{ct} , $E_{ci}(t)$, E_c	Modulus of elasticity at time t							
E_{ci}	Modulus of elasticity at 28 days							
$(f_c')_t$, $f_{cm}(t)$	Compressive strength at time t (psi)							
f_{cm} , f_c'	Compressive strength at 28 days							
H, RH, λ	Relative humidity (%)							
k_f	Concrete strength factor							
k_s , k_c	Size factor							
k_h	Relative humidity factor							
γ_{la}	loading age factor							
γ_λ	relative humidity factor							
γ_{VS}	volume to surface ratio factor							
γ_t	curing time factor	t (days)	1	3	7	14	28	90
		Moist cured	1.2	1.1	1.0	0.93	0.86	0.75
		Steam cured	1.0	0.93	0.86	0.75	-	-
s	cement type factor	RS		N		R		SL
		0.20		0.25		0.25		0.38
t	drying time in days							
t	age of concrete (days)							
t_o	the age of concrete at loading (days)							
t_{la}	loading age in days							
$T(\Delta t_i)$	temperature in Celsius during Δt_i							
Δt_i	number of days where a temperature T prevails							
u	perimeter in contact with the atmosphere							
V/S	Volume to surface ratio in inches							
w_c , *w*	weight of concrete (kcf, pcf respectively)							

Table 3 – Time-line of case study #2

Stage #	Description	Duration (days)
1	Construct abutments and supports, Place beams	0
2	Construction of deck forms	15
3	Casting of CIP slab and pier diaphragms	0
4	Curing of CIP slab and pier diaphragms	28
5	Construction of barrier forms	7
6	Casting of the barriers	0
7	Curing the barriers	28
8	Adding wearing surface	0
9	Curing wearing surface	7
10	Live Load applied	0

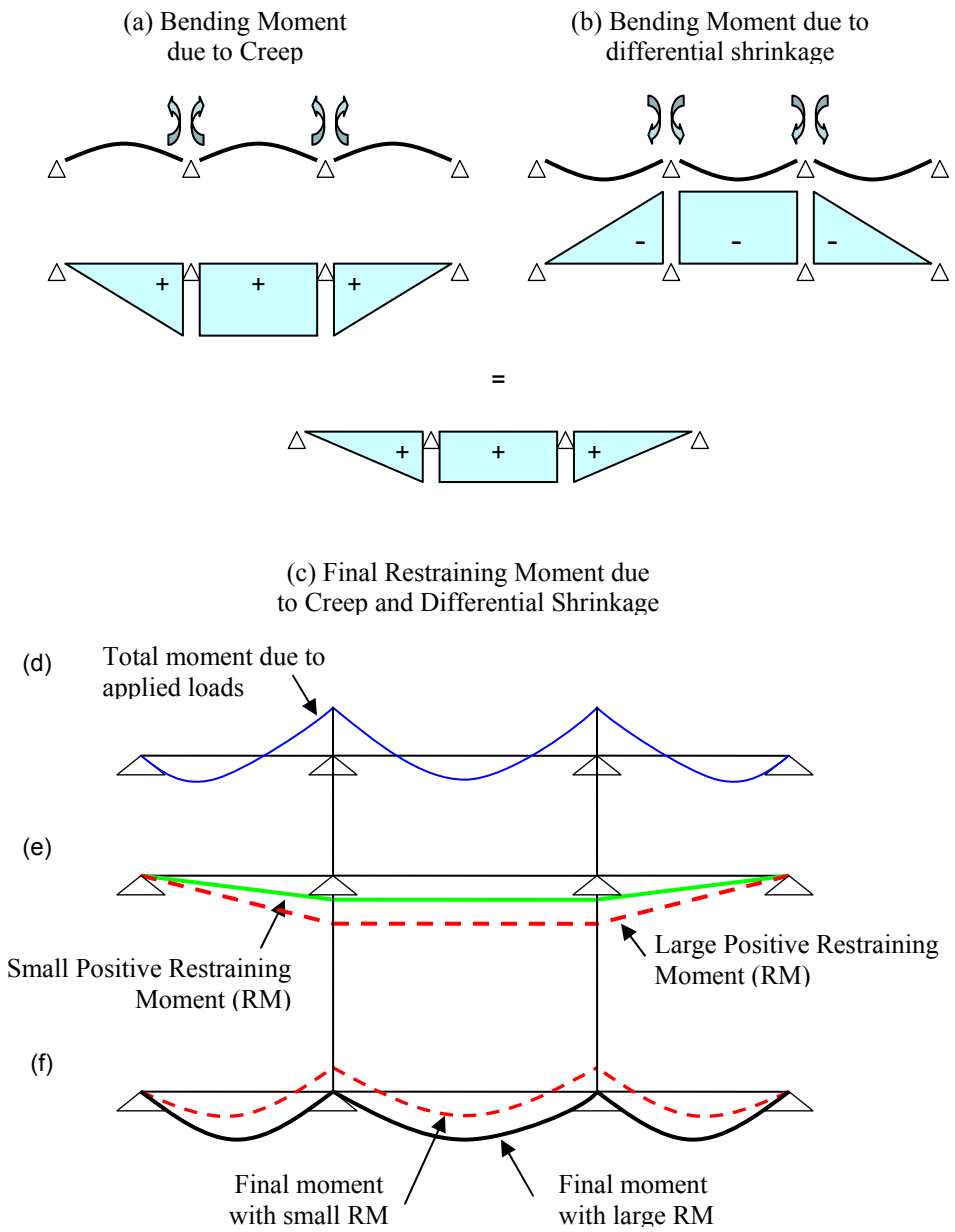

Figure 1 - Effect of creep and shrinkage on composite continuous structures

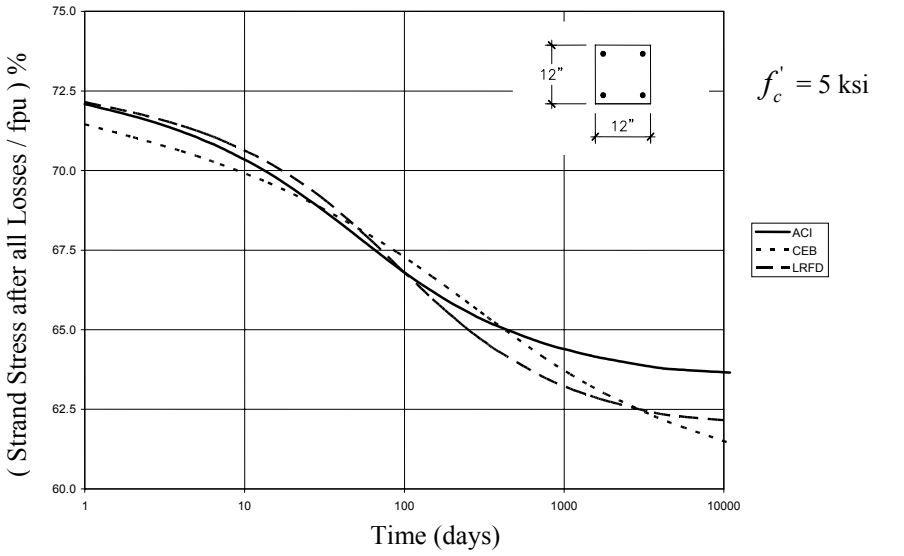

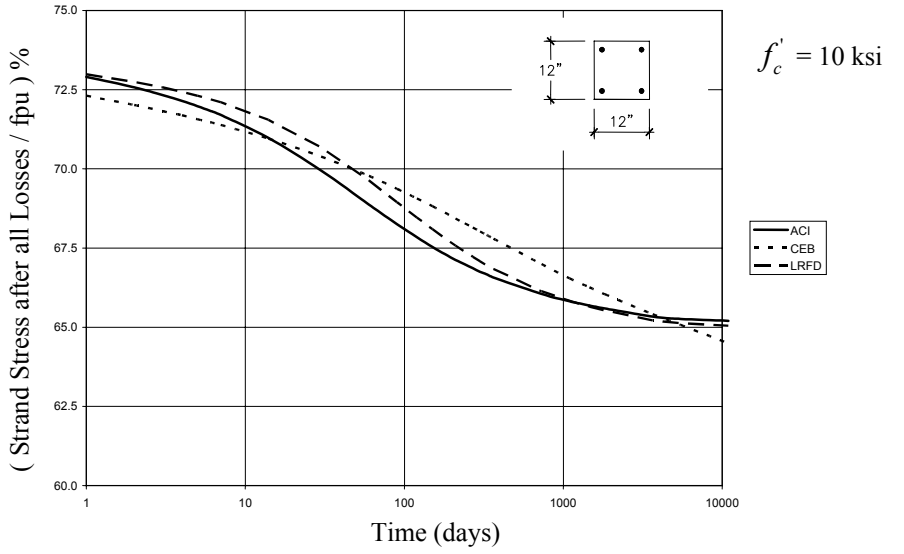

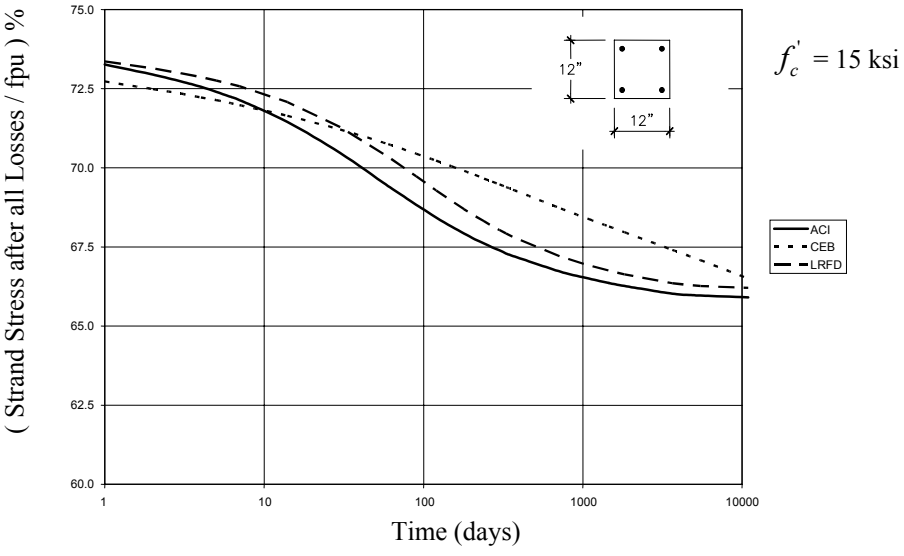

Figure 2 – Case Study #1 (4 – ½" strands)

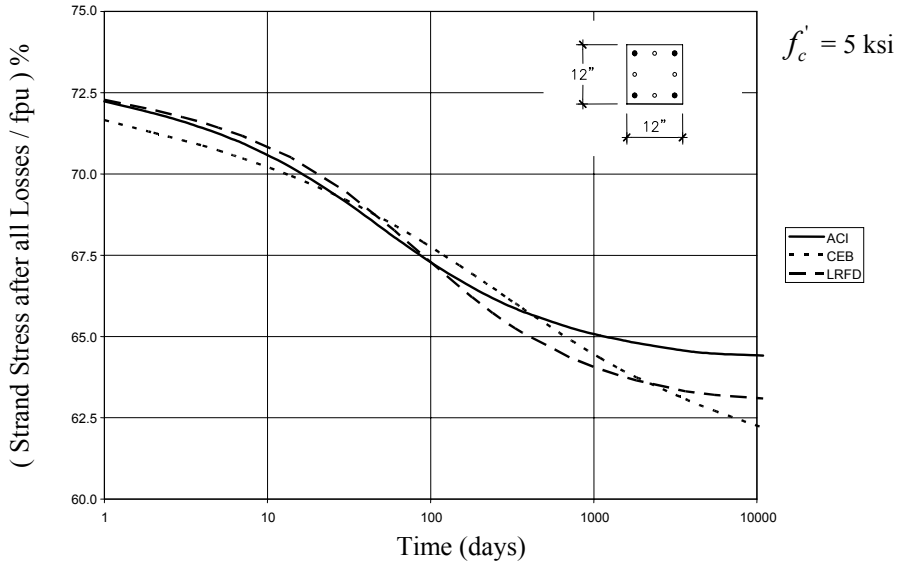

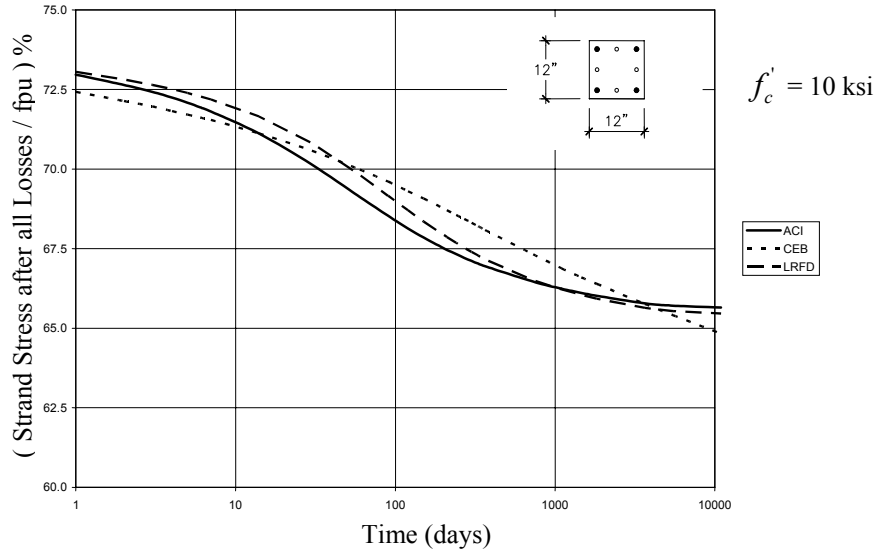

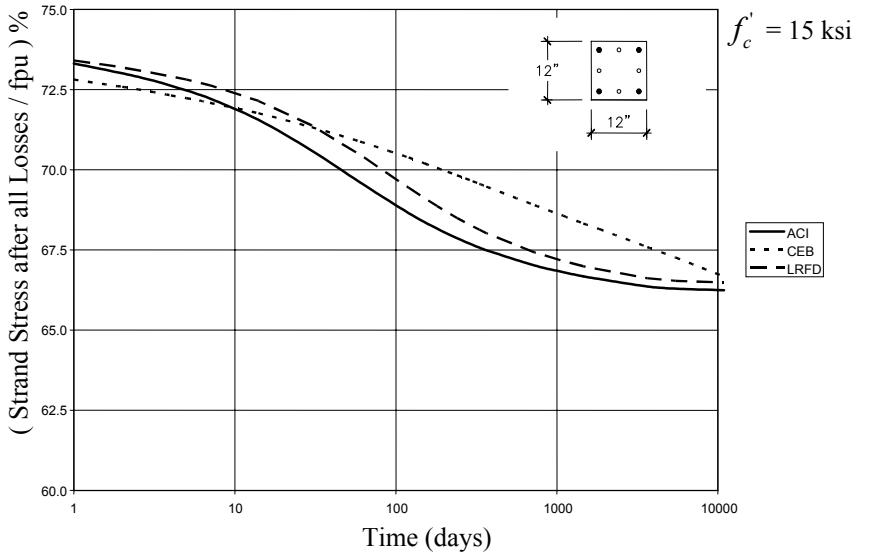

Figure 3 – Case Study #1 (4 – ½" strands + 4 #4 non prestressed bars)

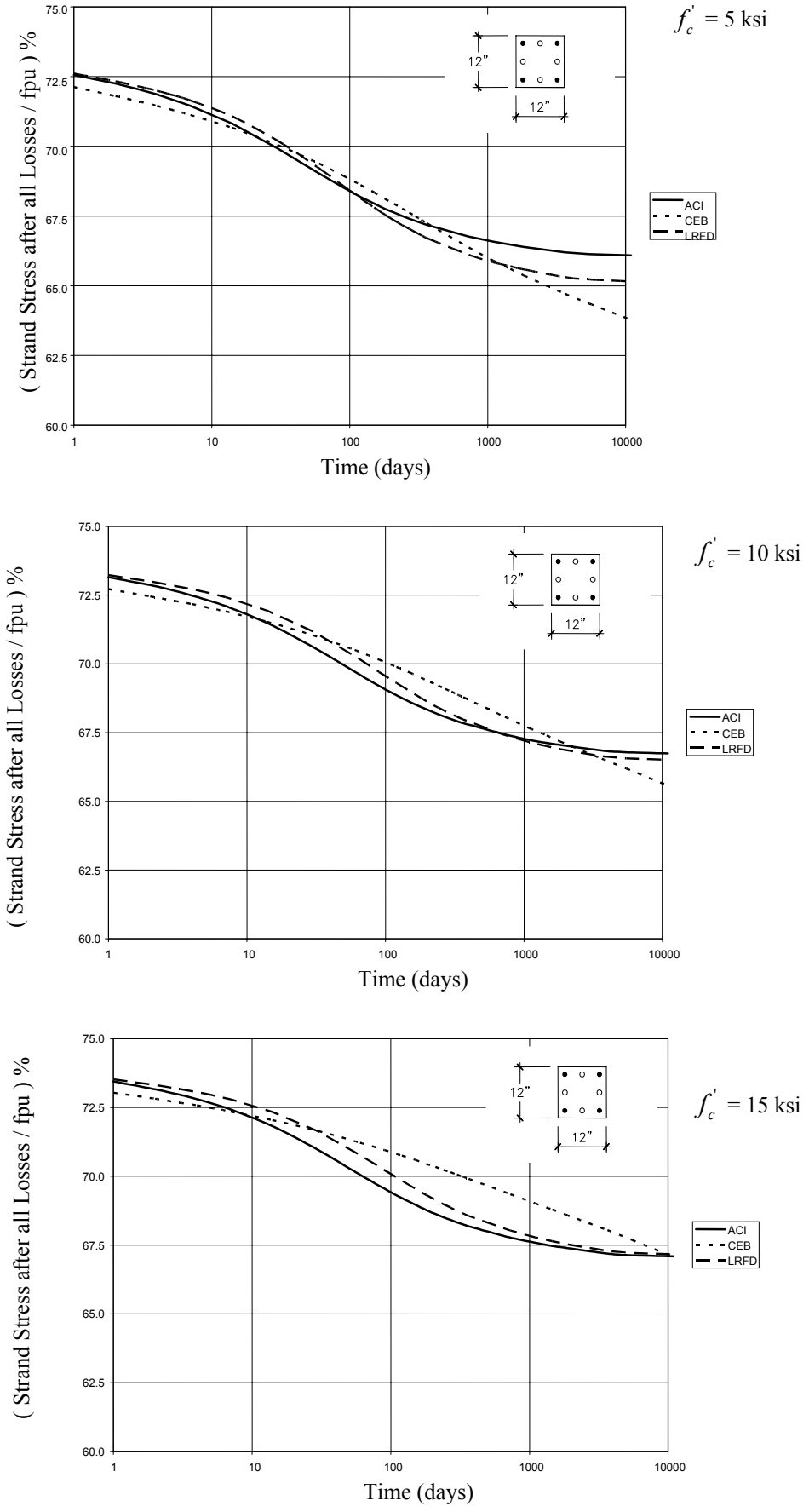

Figure 4 – Case Study #1 (4 – ½" strands + 4 #5 non prestressed bars)

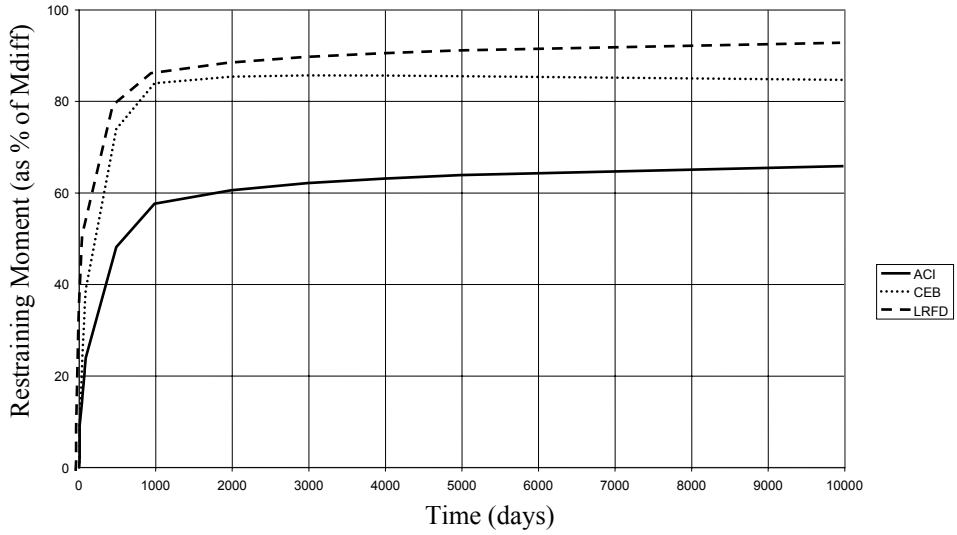

(a) BT - 72 Girder - 30 days old at time of creating continuity

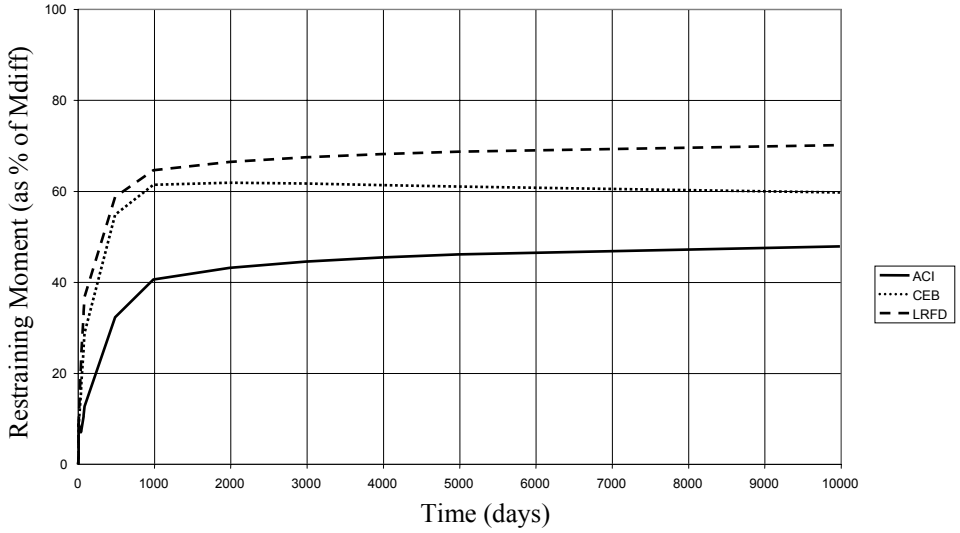

(b) BT - 72 Girder - 60 days old at time of creating continuity

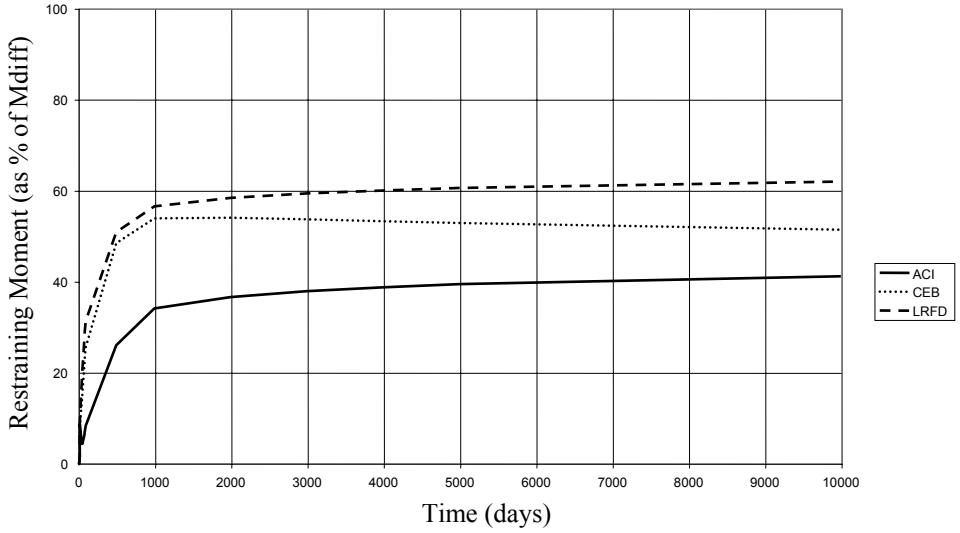

(c) BT - 72 Girder - 90 days old at time of creating continuity

Figure 5 – Restraining moment vs. time for BT 72 Girder

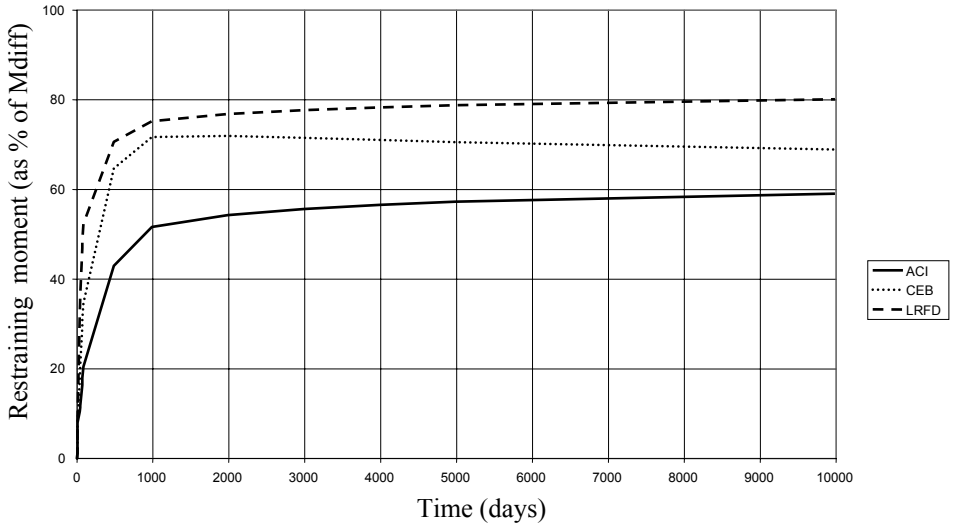

(a) NU1800 Girder - 30 days old at time of creating continuity

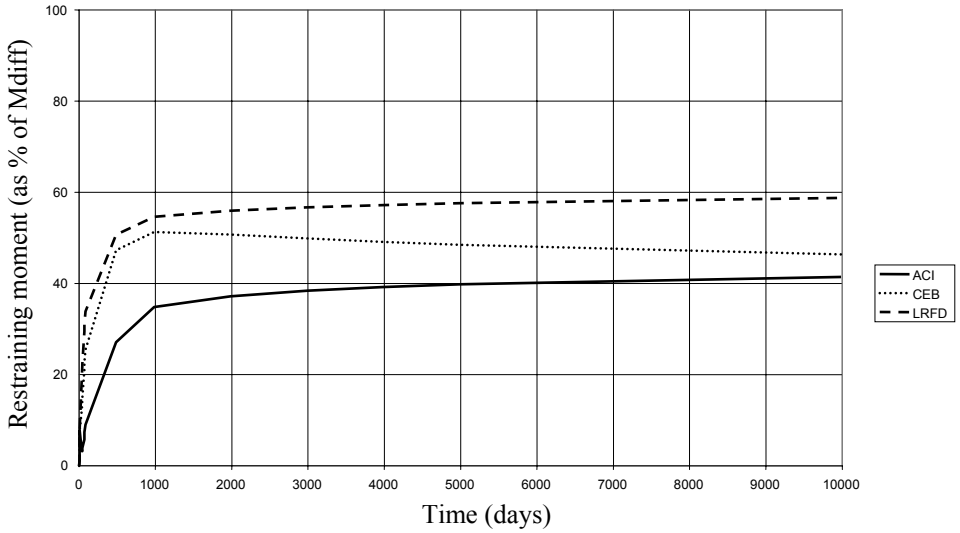

(b) NU1800 Girder - 60 days old at time of creating continuity

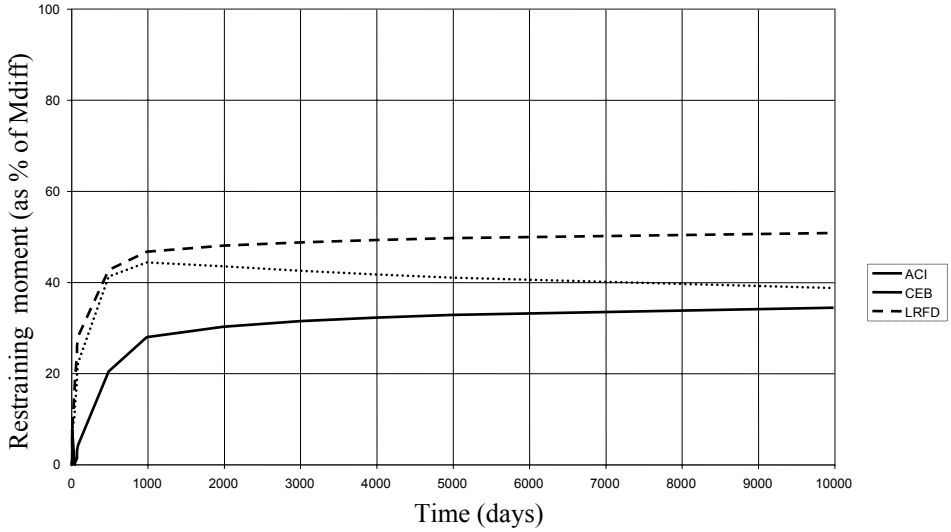

(c) NU1800 Girder - 90 days old at time of creating continuity

Figure 6 – Restraining moment vs. time for NU 1800 Girder

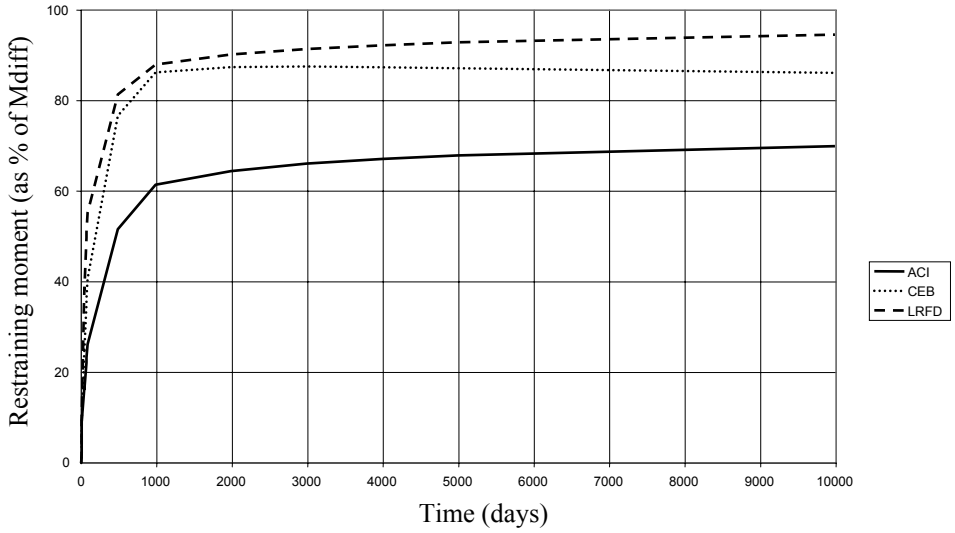

(a) W74G Girder - 30 days old at time of creating continuity

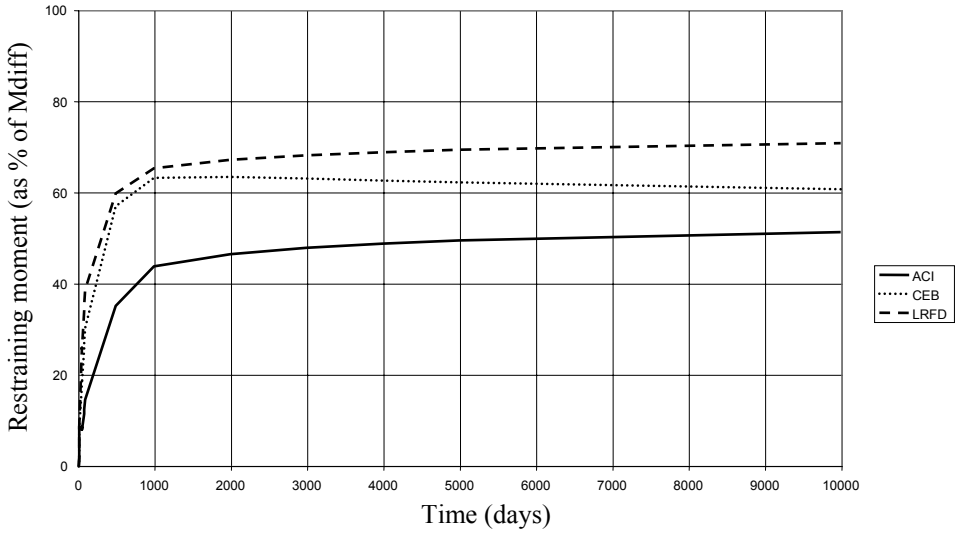

(b) W74G Girder - 60 days old at time of creating continuity

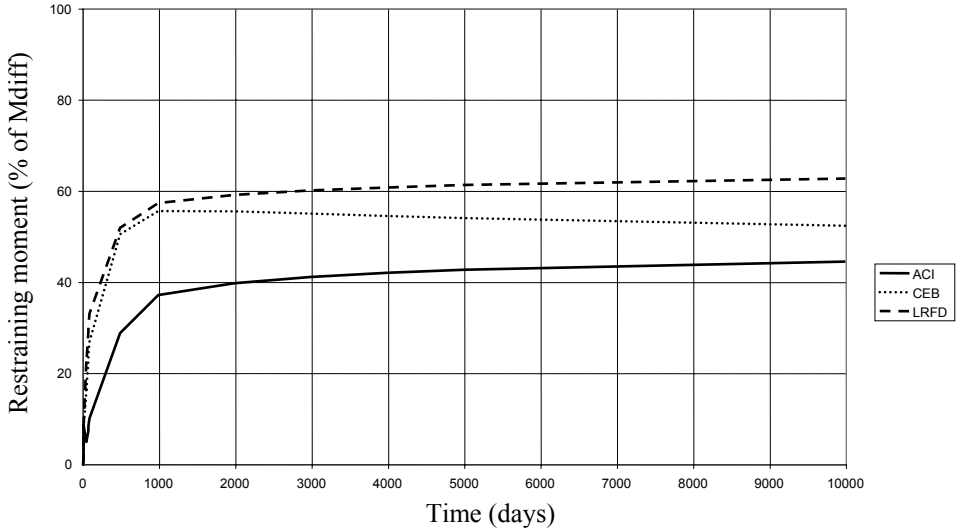

(c) W74G Girder - 90 days old at time of creating continuity

Figure 7 – Restraining moment vs. time for W74G Girder